The Astrophysical Journal Letters, 851:L35 (11pp), 2017 December 20 https://doi.org/10.3847/2041-8213/aa9f0c

GW170608: Observation of a 19 Solar-mass Binary Black Hole Coalescence

LIGO Scientific Collaboration and Virgo Collaboration
(See the end matter for the full list of authors.)

Received 2017 November 14; revised 2017 November 30; accepted 2017 December 2; published 2017 December 18

Abstract

On 2017 June 8 at 02:01:16.49 UTC, a gravitational-wave (GW) signal from the merger of two stellar-mass black holes was observed by the two Advanced Laser Interferometer Gravitational-Wave Observatory detectors with a network signal-to-noise ratio of 13. This system is the lightest black hole binary so far observed, with component masses of $12^{+7}_{-2}\,M_{\odot}$ and $7^{+2}_{-2}\,M_{\odot}$ (90% credible intervals). These lie in the range of measured black hole masses in low-mass X-ray binaries, thus allowing us to compare black holes detected through GWs with electromagnetic observations. The source's luminosity distance is 340^{+140}_{-140} Mpc, corresponding to redshift $0.07^{+0.03}_{-0.03}$. We verify that the signal waveform is consistent with the predictions of general relativity.

Key words: binaries: general – gravitational waves – stars: black holes

1. Introduction

The first detections of binary black hole mergers were made by the Advanced Laser Interferometer Gravitational-Wave Observatory (LIGO; Aasi et al. 2015; Abbott et al. 2016a) during its first observing run (O1) in 2015 (Abbott et al. 2016b, 2016c, 2016d). Following a commissioning break, LIGO undertook a second observing run (O2) from 2016 November 30 to 2017 August 25, with the Advanced Virgo detector (Acernese et al. 2015) joining the run on 2017 August 1. Two binary black hole mergers (Abbott et al. 2017a, 2017b) and one binary neutron star merger (Abbott et al. 2017c) have been reported in O2 data. Here, we describe GW170608, a binary black hole merger with likely the lowest mass of any so far observed by LIGO.

GW170608 was first identified in data from the LIGO Livingston Observatory (LLO), which was in normal observing mode. The LIGO Hanford Observatory (LHO) was operating stably with a sensitivity typical for O2, but its data were not analyzed automatically as the detector was undergoing a routine angular control procedure (Section 2 and the Appendix). Matched-filter analysis of a segment of data around this time revealed a candidate with source parameters consistent between both LIGO detectors; further offline analyses of a longer period of data confirmed the presence of a gravitational-wave (GW) signal from the coalescence of a binary black hole system, with high statistical significance (Section 3).

The source's parameters were estimated via coherent Bayesian analysis (Veitch et al. 2015; Abbott et al. 2016e). A degeneracy between the component masses m_1, m_2 prevents precise determination of their individual values, but the chirp mass $\mathcal{M} = (m_1 m_2)^{3/5}(m_1 + m_2)^{-1/5}$ is well measured and is the smallest so far observed for a merging black hole binary system, with the total mass $M = m_1 + m_2$ also likely the lowest so far observed (Section 4). Individual black hole spins are poorly constrained; however, we find a slight preference for a small positive net component of spin in the direction of the binary orbital angular momentum.

Similarly to GW151226 (Abbott et al. 2016c), this system's black hole component masses are comparable to those of black holes found in X-ray binaries (Section 5) and below those seen in other LIGO–Virgo black hole binaries.

We also test the consistency of the observed GW signal with the predictions of general relativity (GR); we find no deviations from those predictions.

2. Detector Operation

The LIGO detectors measure GW strain using dual-recycled Michelson interferometers with Fabry–Perot arm cavities (Aasi et al. 2015; Abbott et al. 2016a). During O2, the horizon distance for systems with component masses similar to GW170608—the distance at which a binary merger optimally oriented with respect to a detector has an expected signal-to-noise ratio (S/N) of 8 (Allen et al. 2012; Chen et al. 2017)—peaked at ∼1 Gpc for LLO and at ∼750 Mpc for LHO.

At the time of GW170608, LLO was observing with a sensitivity close to its peak. LHO was operating in a stable configuration with a sensitivity of ∼650 Mpc; a routine procedure to minimize angular noise coupling to the strain measurement was being performed (Kasprzack & Yu 2016). Although such times are in general not included in searches, it was determined that LHO strain data were unaffected by the procedure at frequencies above 30 Hz, and may thus be used to identify a GW source and measure its properties. More details on LHO data are given in the Appendix.

Similar procedures to those used in verifying previous GW detections (Abbott et al. 2017b) were followed and indicate that no disturbance registered by LIGO instrumental or environmental sensors (Effler et al. 2015) was strong enough to have caused the GW170608 signal.

Calibration of the LIGO detectors is performed by inducing test-mass motion using photon pressure from modulated auxiliary lasers (Karki et al. 2016; Abbott et al. 2017d; Cahillane et al. 2017). The maximum 1σ calibration uncertainties for strain data used in this analysis are 5% in amplitude and 3° in phase over the frequency range 20–1024 Hz.

The Advanced Virgo detector was, at the time of the event, in observation mode with a horizon distance for signals comparable to GW170608 of 60–70 Mpc. However, this was during an early

commissioning phase with still limited sensitivity; therefore, Virgo data are not included in the analyses presented here.

3. Search for Binary Merger Signals

3.1. Low-latency Identification of a Candidate Event

GW170608 was first identified as a loud (S/N $\sim$ 9) event in LLO data, via visual inspection of single-detector events from a low-latency compact binary matched-filter ("template") analysis (Usman et al. 2016; Nitz et al. 2017a, 2017b). Such events are displayed automatically to diagnose changes in detector operation and in populations of non-Gaussian transient noise artifacts (glitches; Abbott et al. 2016f). Low-latency templated searches (Cannon et al. 2015; Adams et al. 2016; Messick et al. 2017; Nitz et al. 2017b) did not detect the event with high significance because LHO data were not analyzed automatically. An initial investigation of the LLO event did not indicate that it was likely to be caused by an instrumental or environmental artifact (Abbott et al. 2016f; Zevin et al. 2017b). The morphology of the LLO event is consistent with a compact binary merger signal, as shown in Figure 1 (lower panel), but a noise origin could not be ruled out using LLO data alone.

Consequently, LHO data were investigated and were determined to be stable at frequencies above 30 Hz (see the Appendix). A segment of LHO data around the event time was then searched with a filter starting frequency of 30 Hz, using templates approximating the waveforms from compact binary systems with component spins aligned with the orbital angular momentum (Pürrer 2016; Bohé et al. 2017). The fraction of S/N expected to be lost due to imposing the 30 Hz cutoff, as compared to the lower starting frequencies typically used in O2 data (Dal Canton & Harry 2017), is $\sim$1% or less. An event was found having consistent template binary masses and spins, times of arrival, and S/Ns in LHO and LLO. Based on this two-detector coincident event an alert was issued to electromagnetic observing partners 13.5 hr after the event time, with a sky localization (Singer & Price 2016) covering 860 deg^2 (90% credible region). GRB Coordinates Network Circulars related to this event are archived at https://gcn.gsfc.nasa.gov/other/G288732.gcn3.

3.2. Offline Search

To establish the significance of this coincident event, a period between 2017 June 7 and 9 was identified for analysis during which both LIGO interferometers were operating in the same configuration as at the event time. Times at which commissioning activities at LHO produced severe or broadband disturbances in the strain data were excluded from the analysis. Standard offline data quality vetoes for known environmental or instrumental artifacts were also applied, resulting overall in 1.2 days of coincident LHO–LLO data searched.

Two matched-filter pipelines identified GW170608, with a network S/N of 13. A candidate event is assigned a ranking statistic value, in each pipeline, that represents its relative likelihood of originating from a GW signal *versus* from noise. One pipeline estimates the noise background using time-shifted data (Usman et al. 2016) and limits the rate of occurrence of noise events ranked higher than GW170608 to less than 1 in 3000 years. This limit arises from the maximum background analysis time available from time shifts separated by 0.1 s and is expected to be conservative as indicated by previous studies (Was et al. 2010; Abbott et al. 2016g; Capano et al. 2017). The other pipeline uses different methods for ranking candidate events and for estimating the background

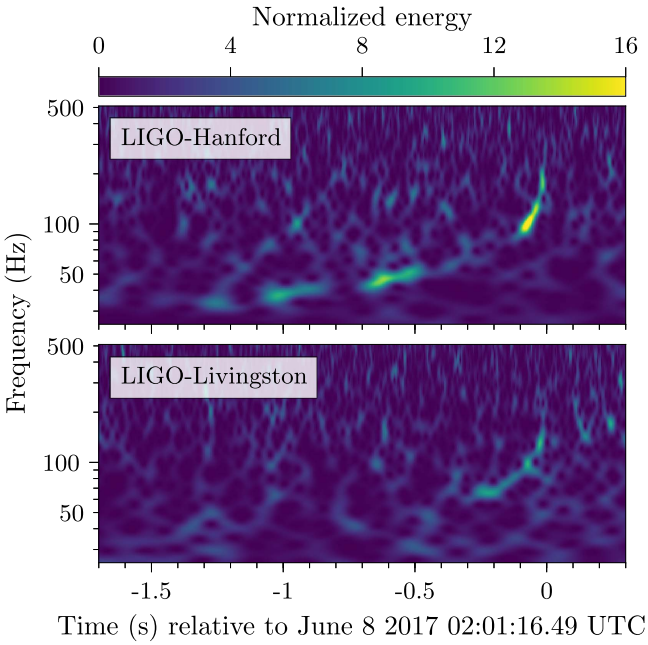

Figure 1. Power maps of LIGO strain data at the time of GW170608 in a constant Q sine-Gaussian basis (Chatterji et al. 2004). The characteristic upward-chirping morphology of a binary inspiral driven by GW emission is visible in both detectors, with a higher signal amplitude in LHO. This figure, and all others in this Letter, were produced from noise-subtracted data (Section 4).

(Cannon et al. 2015; Messick et al. 2017) and assigns the event a false-alarm rate of 1 in 160,000 years.

A search for transient GW signals coherent between LHO and LLO with frequency increasing over time, without using waveform templates (Klimenko et al. 2016), also identified GW170608 with a false-alarm rate of 1 in $\sim$30 years; the lower significance is expected as this analysis is typically less sensitive to lower-mass compact binary signals than matched-filter searches.

4. Source Properties

4.1. Binary Parameters

The parameters of the GW source are inferred from a coherent Bayesian analysis (Veitch et al. 2015; Abbott et al. 2016e) using noise-subtracted data from the two LIGO observatories. Several continuously present sources of noise in the detectors' GW strain channel are independently measured, and are then subtracted via Wiener filtering (Abbott et al. 2017b and references therein). This step increases the expected S/N of compact binary signals in LHO data typically by 25% (Driggers et al. 2017). The likelihood integration is performed starting at 30 Hz in LHO and 20 Hz in LLO, includes marginalization over strain calibration uncertainties (Farr et al. 2015), and uses the noise power spectral densities (Littenberg & Cornish 2015) at the time of the event.

Two different GW signal models calibrated to numerical relativity simulations of general relativistic binary black hole mergers (Mroué et al. 2013; Chu et al. 2016; Husa et al. 2016), building on the breakthrough reported in Pretorius (2005), Baker et al. (2006), and Campanelli et al. (2006), are used. One waveform family models the inspiral-merger-ringdown signal of precessing binary black holes (Hannam et al. 2014), which includes spin-induced orbital precession through a transformation of the aligned-spin waveform model of Husa et al. (2016) and Khan et al. (2016); we refer to this model as the *effective precession* model. The other waveform model describes binaries

Table 1
Source Properties for GW170608

Chirp mass $\mathcal{M}$	$7.9^{+0.2}_{-0.2}\,M_\odot$
Total mass M	$19^{+5}_{-1}\,M_\odot$
Primary black hole mass m_1	$12^{+7}_{-2}\,M_\odot$
Secondary black hole mass m_2	$7^{+2}_{-2}\,M_\odot$
Lower bound on mass ratio m_2/m_1	0.33
Effective inspiral spin parameter $\chi_{\rm eff}$	$0.07^{+0.23}_{-0.09}$
Final black hole mass $M_{\rm f}$	$18.0^{+4.8}_{-0.9}\,M_\odot$
Final black hole spin $a_{\rm f}$	$0.69^{+0.04}_{-0.05}$
Radiated energy $E_{\rm rad}$	$0.85^{+0.07}_{-0.17}\,M_\odot c^2$
Peak luminosity $\ell_{\rm peak}$	$3.4^{+0.5}_{-1.6}\times 10^{56}$ erg s^{-1}
Luminosity distance $D_{\rm L}$	340^{+140}_{-140} Mpc
Source redshift z	$0.07^{+0.03}_{-0.03}$

Note. We quote median values with 90% credible intervals (90% bound on mass ratio). Source-frame masses are quoted; to convert to detector frame, multiply by $(1+z)$ (Krolak & Schutz 1987). The redshift assumes a flat cosmology with Hubble parameter $H_0 = 67.9$ km s^{-1} Mpc^{-1} and matter density parameter $\Omega_{\rm m} = 0.3065$ (Ade et al. 2016).

with spin angular momenta aligned with the orbital angular momentum (Pürrer 2016; Bohé et al. 2017), henceforth referred to as *non-precessing*. For their common parameters, both waveform models yield consistent parameter ranges.

A selection of inferred source parameters for GW170608 is given in Table 1; unless otherwise noted, we report median values and symmetric 90% credible intervals. The quoted parameter uncertainties include statistical and systematic errors from averaging posterior probability samples over the two waveform models. As in Abbott et al. (2017a), our estimates of the mass and spin of the final black hole, the total energy radiated in GWs, as well as the peak luminosity are computed from fits to numerical relativity simulations (Hofmann et al. 2016; Healy & Lousto 2017; Jiménez-Forteza et al. 2017; Keitel et al. 2017).

The posterior probability distributions for the source-frame mass parameters of GW170608 are shown in Figure 2, together with those for GW151226 (Abbott et al. 2016c). The initial binary of GW170608 had source-frame component masses $m_1 = 12^{+7}_{-2}\,M_\odot$ and $m_2 = 7^{+2}_{-2}\,M_\odot$. As with previously reported binary merger GW signals, GW170608's data are consistent with an equal-mass binary; the mass ratio is loosely constrained to $m_2/m_1 > 0.33$. Since neutron stars are expected to have masses below $\sim 3\,M_\odot$ (Lattimer & Prakash 2016), both objects are most likely black holes.

Notably, we find this binary black hole system to be the least massive yet observed through GWs. The next lightest, GW151226 (Abbott et al. 2016c), has a chirp mass $\mathcal{M} = 8.9^{+0.3}_{-0.3}$ and a total mass $M = 21.8^{+5.9}_{-1.7}$, compared to values of $\mathcal{M} = 7.9^{+0.2}_{-0.2}\,M_\odot$ and $M = 19^{+5}_{-1}\,M_\odot$ for GW170608. The probability that GW170608's total mass is smaller than GW151226's is 0.89.

While the chirp mass is tightly constrained, spins have a more subtle effect on the GW signal. The effective inspiral spin $\chi_{\rm eff}$, a mass-weighted combination of the spin components (anti-)aligned with the orbital angular momentum (Racine 2008; Ajith et al. 2011), predominantly affects the inspiral rate of the binary but also influences the merger. We infer that $\chi_{\rm eff} = 0.07^{+0.23}_{-0.09}$, disfavoring large, anti-aligned spins on both black holes.

An independent parameter estimation method comparing LIGO strain data to hybridized numerical relativity simulations

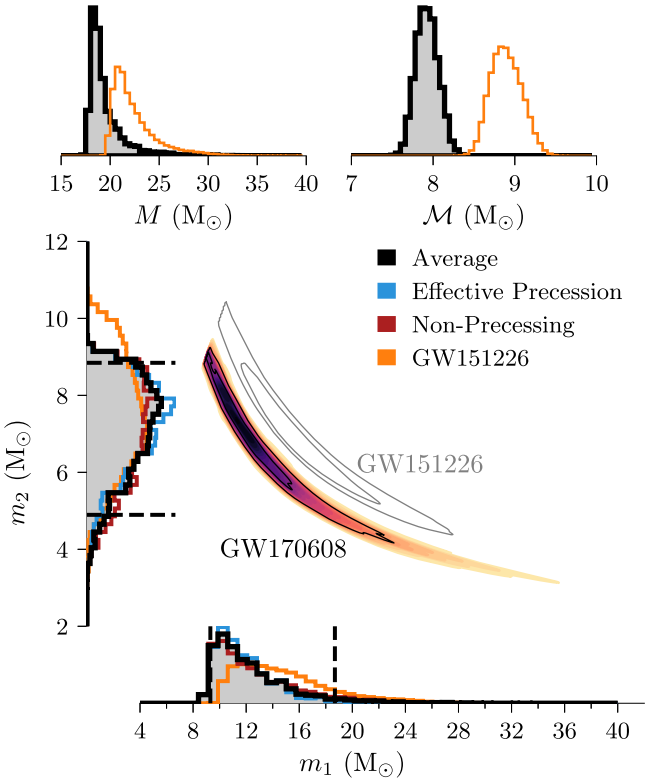

Figure 2. Posterior probability densities for binary component masses (m_1, m_2), total mass (M), and chirp mass ($\mathcal{M}$) in the source frame. One-dimensional component mass distributions include posteriors for the effective precession (blue) and the non-precessing (red) waveform model, as well as their average (black). The dashed lines demarcate the 90% credible intervals for the average posterior. The two-dimensional plot shows contours of the 50% and 90% credible regions overlaid on a color-coded posterior density function. For comparison, we show both one- and two-dimensional distributions of averaged component mass posterior samples for GW151226 (orange; Abbott et al. 2016c). In the top panel, we further compare GW170608 and GW151226's source-frame total mass (left) and source-frame chirp mass (right). All other known binary black holes lie at higher chirp masses than GW170608 and GW151226.

of binary black hole systems with non-precessing spins (Abbott et al. 2016h) yields estimates of component masses and $\chi_{\rm eff}$ consistent with our model-waveform analysis.

Spin components orthogonal to the orbital angular momentum are the source of precession (Apostolatos et al. 1994; Kidder 1995) and may be parameterized by a single effective precession spin χ_p (Schmidt et al. 2015). For precessing binaries, component spin orientations evolve over time; we report results evolved to a reference GW frequency of 20 Hz. The spin prior assumed in this analysis is uniform in dimensionless spin magnitudes $\boldsymbol{\chi}_i \equiv c|\boldsymbol{S}|_i/(Gm_i^2)$ with $i = 1, 2$ between 0 and 0.89 and isotropic in their orientation; this prior on component spins maps to priors for the effective parameters $\chi_{\rm eff}$ and χ_p. The top panel of Figure 3 shows the prior and posterior probability distributions of $\chi_{\rm eff}$ and χ_p obtained for the effective precession waveform model. While we gain some information about $\chi_{\rm eff}$, the χ_p posterior is dominated by its prior, thus we cannot draw any strong conclusion on the size of spin components in the orbital plane. Previous GW events also yielded little information on in-plane spins (Abbott et al. 2016b, 2016c, 2017a); possible effects of prior choice on this inference were investigated in Vitale et al. (2017a). The inferred component spin magnitudes and orientations are shown in the bottom panel of Figure 3. We find the dimensionless spin magnitude of the primary black hole, χ_1, to be less than 0.75

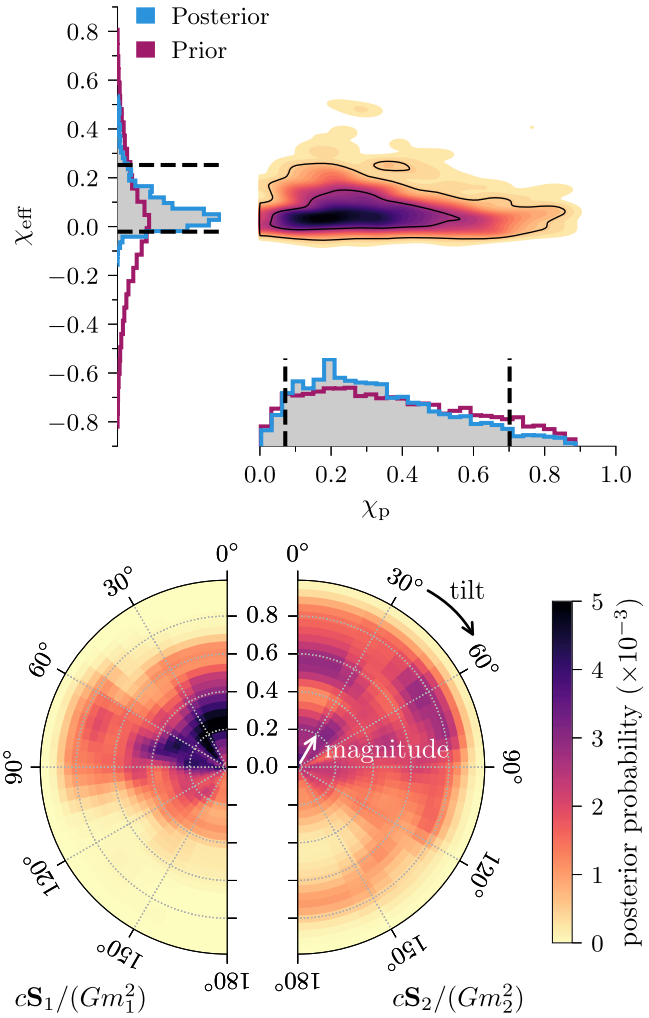

Figure 3. Top panel: marginalized one-dimensional posterior density functions for the spin parameters χ_p and $\chi_{\rm eff}$ (blue) in comparison to their prior distributions (pink) as obtained from the effective precession model. The dashed lines indicate the 90% credible interval. The two-dimensional plot shows the 50% and 90% credible regions plotted over the posterior density function. Bottom panel: posterior probabilities for the dimensionless component spins $\boldsymbol{\chi}_i$ with $i = 1, 2$ relative to the Newtonian orbital angular momentum $\hat{\boldsymbol{L}}$, i.e., the normal of the orbital plane. The tilt angles are 0° for spins parallel to $\hat{\boldsymbol{L}}$ and 180° for spins anti-parallel to $\hat{\boldsymbol{L}}$. The posterior density functions are marginalized over the azimuthal angles. Each pixel has a prior probability of $\sim 1.8 \times 10^{-3}$; they are spaced linearly in spin magnitudes and the cosine of the tilt angles.

(90% credible limit); this limit is robust to extending the prior range of spin magnitudes and to using different waveform models.

The measurability of precession depends on the intrinsic source properties as well as the angle of the binary orbital angular momentum to the line of sight (i.e., inclination). The inclination of GW170608's orbit is likely close to either 0° or 180°, due to a selection effect: the distance inside which a given binary merger would be detectable at a fixed S/N threshold is largest for these inclination values (Schutz 2011). For such values, the waveform carries little information on precession.

The distance of GW170608 is extracted from the observed signal amplitude given the binary's inclination (Abbott et al. 2016e). With the network of two nearly co-aligned LIGO detectors, the uncertainty on inclination translates into a large distance uncertainty: we infer a luminosity distance of $D_L = 340^{+140}_{-140}$ Mpc, corresponding to a redshift of $z = 0.07^{+0.03}_{-0.03}$ assuming a flat ΛCDM cosmology (Ade et al. 2016).

GW170608 is localized to a sky area of $\sim$520 deg^2 in the northern hemisphere (90% credible region), determined largely by the signal's measured arrival time at LLO $\sim$ 7 ms later than at LHO. This reduction in area relative to the low-latency map is partly attributable to the use of noise-subtracted data with offline calibration (Abbott et al. 2017b).

4.2. Consistency with General Relativity

To test whether GW170608 is consistent with the predictions of GR, we consider possible deviations of coefficients describing the binary inspiral part of the signal waveform from the values expected in GR, as was done for previous detections (Abbott et al. 2016d, 2016i, 2017a). Tests involving parameters describing the merger and ringdown do not yield informative results, since the merger happens at relatively high frequency where the LIGO detectors are less sensitive. As in Abbott et al. (2017b), we also allow a sub-leading phase contribution at effective −1PN order, i.e., with a frequency dependence of $f^{-7/3}$, which is absent in GR. The GR predicted value is contained within the 90% credible interval of the posterior distribution for all parameters tested.

Assuming that gravitons are dispersed in vacuum similarly to massive particles, we also obtained an upper bound on the mass of the graviton comparable to the constraints previously obtained (Abbott et al. 2016b, 2016i, 2017a). Possible violations of local Lorentz invariance, manifested via modifications to the GW dispersion relation, were investigated (Abbott et al. 2017a), again finding upper bounds comparable to previous results.

5. Astrophysical Implications

The low mass of GW170608's source binary, in comparison to other binary black hole systems observed by LIGO and Virgo, has potential implications for the binary's progenitor environment. High-metallicity progenitors are expected to experience substantial mass loss through strong stellar winds, while less mass loss is exhibited for low-metallicity progenitors (Belczynski et al. 2010; Spera et al. 2015). Thus, unlike more massive black hole binaries, GW170608's low component masses do not necessarily require formation at low metallicity. Further discussion of the relationship between black hole masses and metallicity can be found in Abbott et al. (2016j).

We may compare GW170608's relatively low-mass black hole binary components to black holes found in X-ray binaries. X-ray binary systems contain either a black hole or neutron star that accretes matter from a companion donor star. Low-mass X-ray binaries (LMXBs) are X-ray binaries with a low-mass donor star that transfer mass through Roche lobe overflow (Charles & Coe 2003). The inferred component masses of GW170608 are consistent with dynamically measured masses of black holes found in LMXBs, typically less than 10 $M_\odot$ (Özel et al. 2010; Farr et al. 2011; Corral-Santana et al. 2016).

Binary black holes may form through many different channels, including, but not limited to, dynamical interaction (Mapelli 2016; O'Leary et al. 2016; Rodriguez et al. 2016) and isolated binary evolution (Belczynski et al. 2016; Eldridge & Stanway 2016; Lipunov et al. 2017; Stevenson et al. 2017b). While the inferred masses and tilt measurements of GW170608 are not sufficiently constrained to favor a formation channel, future measurements of binary black hole systems may hint at the formation histories of such systems (Abbott et al. 2017a, 2016j and references therein). It may be possible to determine the relative proportion of binaries originating in each canonical formation channel following $\mathcal{O}(100)$

binary black hole detections (Farr et al. 2017a; Farr et al. 2017b; Stevenson et al. 2017a; Talbot & Thrane 2017; Vitale et al. 2017b; Zevin et al. 2017a).

The detection of GW170608 is consistent with the merger populations considered in Abbott et al. (2016k, 2016d), for which a rate of 12–213 $\mathrm{Gpc}^{-3}\ \mathrm{yr}^{-1}$ was estimated in Abbott et al. (2017a).

6. Outlook

LIGO's detection of GW170608 extends the mass range of known stellar-mass binary black hole systems and hints at connections with other known astrophysical systems containing black holes. The O2 run ended on 2017 August 25; a full catalog of binary merger GW events for this run is in preparation, including candidate signals with lower significance and systems other than stellar-mass black hole binaries (Abbott et al. 2017c). Estimates of the merger rate and mass distribution for the emerging compact binary population will also be updated.

With expected increases in detector sensitivity in the third advanced detector network observing run, projected for late 2018 (Abbott et al. 2016l), detection of black hole binaries will be a routine occurrence; studying this population will eventually answer many questions about these systems' origins and evolution.

The authors gratefully acknowledge the support of the United States National Science Foundation (NSF) for the construction and operation of the LIGO Laboratory and Advanced LIGO as well as the Science and Technology Facilities Council (STFC) of the United Kingdom, the Max-Planck-Society (MPS), and the State of Niedersachsen/Germany for support of the construction of Advanced LIGO and construction and operation of the GEO600 detector. Additional support for Advanced LIGO was provided by the Australian Research Council. The authors gratefully acknowledge the Italian Istituto Nazionale di Fisica Nucleare (INFN), the French Centre National de la Recherche Scientifique (CNRS) and the Foundation for Fundamental Research on Matter supported by the Netherlands Organisation for Scientific Research, for the construction and operation of the Virgo detector and the creation and support of the EGO consortium. The authors also gratefully acknowledge research support from these agencies as well as by the Council of Scientific and Industrial Research of India, the Department of Science and Technology, India, the Science & Engineering Research Board (SERB), India, the Ministry of Human Resource Development, India, the Spanish Agencia Estatal de Investigación, the Vicepresidència i Conselleria d'Innovació Recerca i Turisme and the Conselleria d'Educació i Universitat del Govern de les Illes Balears, the Conselleria d'Educació Investigació Cultura i Esport de la Generalitat Valenciana, the National Science Centre of Poland, the Swiss National Science Foundation (SNSF), the Russian Foundation for Basic Research, the Russian Science Foundation, the European Commission, the European Regional Development Funds (ERDF), the Royal Society, the Scottish Funding Council, the Scottish Universities Physics Alliance, the Hungarian Scientific Research Fund (OTKA), the Lyon Institute of Origins (LIO), the National Research, Development and Innovation Office Hungary (NKFI), the National Research Foundation of Korea, Industry Canada and the Province of Ontario through the Ministry of Economic Development and Innovation, the Natural Science and Engineering Research Council Canada, the Canadian Institute for Advanced Research, the Brazilian Ministry of Science, Technology, Innovations, and Communications, the International Center for Theoretical Physics South American Institute for Fundamental Research (ICTP-SAIFR), the Research Grants Council of Hong Kong, the National Natural Science Foundation of China (NSFC), the Leverhulme Trust, the Research Corporation, the Ministry of Science and Technology (MOST), Taiwan and the Kavli Foundation. The authors gratefully acknowledge the support of the NSF, STFC, MPS, INFN, CNRS and the State of Niedersachsen/Germany for provision of computational resources.

Appendix
Angular Coupling Minimization

GW170608 was observed during a routine instrumental procedure at LHO that minimizes the coupling of angular control of the test masses to noise in the GW strain measurement. To maintain resonant power in the arms, the pitch and yaw angular degrees of freedom of the four suspended cavity test masses at each detector (Abbott et al. 2016a) must be controlled. This is achieved by actuating on the second stage of the LIGO quadruple suspensions. A feed-forward control is employed in order to leave the beam position of the main laser on the test mass unchanged while this actuation is applied. However, if this position differs from the actuation point, the angular control can affect the differential arm length, thus introducing additional noise in the strain measurement (Kasprzack & Yu 2016). As the beam position can drift over periods of hours or days, the angular feed-forward control must be periodically adjusted in order to minimize the coupling to strain.

During this procedure, high amplitude pitch and yaw excitations are applied to the test masses via actuation of the suspensions. Each of the 8 angular degrees of freedom is excited at a distinct frequency; the resulting length signals are observed via demodulation at each excitation frequency, revealing how strongly the corresponding degree of freedom couples to differential arm length. The feed-forward gain settings are stepped at intervals of approximately 45 s and the global minimum of angular control coupling to strain is determined from the resulting measurements. The frequencies of angular excitations are equally spaced between ∼19 Hz and ∼23 Hz, generating excess power in the differential arm motion, and thus in the measured strain around these frequencies. This procedure covers from ∼2 minutes before to ∼14 minutes after GW170608, shown in Figure 4 (left). During the period from −2 to 2 minutes, substantial excess noise is visible at frequencies around 20 Hz. To characterize this noise we show amplitude spectral densities derived from 240 s of data both before the onset of the angular excitations and during the excitations around the event time in Figure 4 (right). No effect on the spectrum is visible above 30 Hz.

During the procedure, angular control gain settings are stepped abruptly; inspection of all such transition times shows no evidence for transient excess noise in the strain data outside the 19–23 Hz excitation band. The closest transition to the event time was 10 s before the binary merger; thus, any transient noise associated with this transition could not have affected the matched-filter output at the event time (template waveforms for GW170608-like signals have a duration between 2 and 3 s). Furthermore, the output of a matched-filter search analyzing LHO data from periods when this procedure was performed shows a distribution of S/Ns similar to that obtained from other times. Thus, we find no evidence that the angular coupling minimization affected the recorded strain data at LHO around the event time at frequencies above 30 Hz.

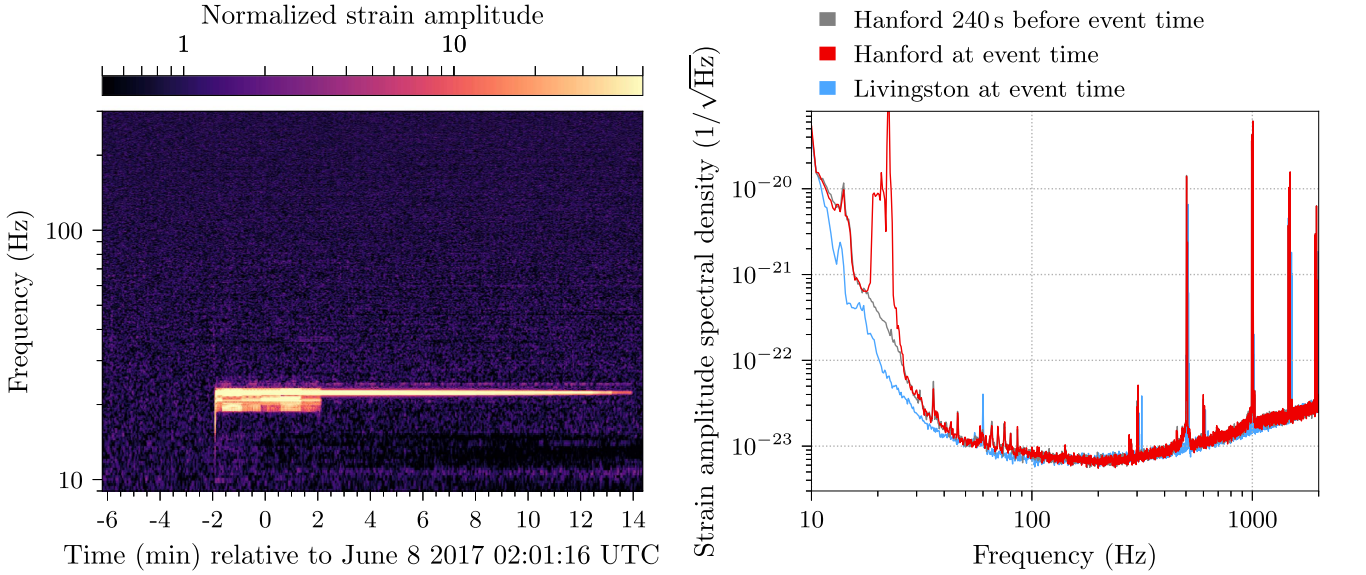

Figure 4. Left: spectrogram of strain data from LHO around the time of GW170608. This plot shows variations in the noise spectrum of the detector over periods on the scale of minutes; unlike Figure 1, it is not designed to show short-duration transient events. The strain amplitude is normalized to the interval between −6 and −2 minutes relative to the event time. See the Appendix for a discussion of the feature around 20 Hz due to an angular control procedure. Right: amplitude spectral density of strain data at both LIGO observatories for 240 s around the event time, (−2, 2) minutes in the left panel, and for data before the start of the angular coupling minimization at LHO, (−6, −2) minutes. Excess noise is clearly visible around 20 Hz but data above 30 Hz are unaffected.

References

Aasi, J., Abadie, J., Abbott, B. P., et al. 2015, CQGra, 32, 074001
Abbott, B. P., Abbott, R., Abbott, T. D., et al. 2016a, PhRvL, 116, 131103
Abbott, B. P., Abbott, R., Abbott, T. D., et al. 2016b, PhRvL, 116, 061102
Abbott, B. P., Abbott, R., Abbott, T. D., et al. 2016c, PhRvL, 116, 241103
Abbott, B. P., Abbott, R., Abbott, T. D., et al. 2016d, PhRvX, 6, 041015
Abbott, B. P., Abbott, R., Abbott, T. D., et al. 2016e, PhRvL, 116, 241102
Abbott, B. P., Abbott, R., Abbott, T. D., et al. 2016f, CQGra, 33, 134001
Abbott, B. P., Abbott, R., Abbott, T. D., et al. 2016g, PhRvD, 93, 122003
Abbott, B. P., Abbott, R., Abbott, T. D., et al. 2016h, PhRvD, 94, 064035
Abbott, B. P., Abbott, R., Abbott, T. D., et al. 2016i, PhRvL, 116, 221101
Abbott, B. P., Abbott, R., Abbott, T. D., et al. 2016j, ApJL, 818, L22
Abbott, B. P., Abbott, R., Abbott, T. D., et al. 2016k, ApJL, 833, L1
Abbott, B. P., Abbott, R., Abbott, T. D., et al. 2016l, LRR, 19, 1
Abbott, B. P., Abbott, R., Abbott, T. D., et al. 2017a, PhRvL, 118, 221101
Abbott, B. P., Abbott, R., Abbott, T. D., et al. 2017b, PhRvL, 119, 141101
Abbott, B. P., Abbott, R., Abbott, T. D., et al. 2017c, PhRvL, 119, 161101
Abbott, B. P., Abbott, R., Abbott, T. D., et al. 2017d, PhRvD, 95, 062003
Acernese, F., Agathos, M., Agatsuma, K., et al. 2015, CQGra, 32, 024001
Adams, T., Buskulic, D., Germain, V., et al. 2016, CQGra, 33, 175012
Ade, P. A. R., Aghanim, N., Arnaud, M., et al. 2016, A&A, 594, A13
Ajith, P., Hannam, M., Husa, S., et al. 2011, PhRvL, 106, 241101
Allen, B., Anderson, W. G., Brady, P. R., Brown, D. A., & Creighton, J. D. E. 2012, PhRvD, 85, 122006
Apostolatos, T. A., Cutler, C., Sussman, G. J., & Thorne, K. S. 1994, PhRvD, 49, 6274
Baker, J. G., Centrella, J., Choi, D.-I., Koppitz, M., & van Meter, J. 2006, PhRvL, 96, 111102
Belczynski, K., Bulik, T., Fryer, C. L., et al. 2010, ApJ, 714, 1217
Belczynski, K., Holz, D. E., Bulik, T., & O'Shaughnessy, R. 2016, Natur, 534, 512
Bohé, A., Shao, L., Taracchini, A., et al. 2017, PhRvD, 95, 044028
Cahillane, C., Betzwieser, J., Brown, D. A., et al. 2017, PhRvD, 96, 102001
Campanelli, M., Lousto, C. O., Marronetti, P., & Zlochower, Y. 2006, PhRvL, 96, 111101
Cannon, K., Hanna, C., & Peoples, J. 2015, arXiv:1504.04632
Capano, C., Dent, T., Hanna, C., et al. 2017, PhRvD, 96, 082002
Charles, P. A., & Coe, M. J. 2003, arXiv:astro-ph/0308020
Chatterji, S., Blackburn, L., Martin, G., & Katsavounidis, E. 2004, CQGra, 21, S1809
Chen, H.-Y., Holz, D. E., Miller, J., et al. 2017, arXiv:1709.08079
Chu, T., Fong, H., Kumar, P., et al. 2016, CQGra, 33, 165001
Corral-Santana, J. M., Casares, J., Munoz-Darias, T., et al. 2016, A&A, 587, A61
Dal Canton, T., & Harry, I. 2017, arXiv:1705.01845
Driggers, J. C., Dwyer, S., Effler, A., et al. 2017, Improving Astrophysical Parameter Estimation via Offline Noise Subtraction for Advanced LIGO, Tech. Rep. LIGO-P1700260, https://dcc.ligo.org/LIGO-P1700260/public
Effler, A., Schofield, R. M. S., Frolov, V. V., et al. 2015, CQGra, 32 035017
Eldridge, J. J., & Stanway, E. R. 2016, MNRAS, 462, 3302
Farr, B., Holz, D. E., & Farr, W. M. 2017a, arXiv:1709.07896
Farr, W. M., Farr, B., Littenberg, T. & LIGO Scientific Collaboration and Virgo Collaboration 2015, Modelling Calibration Errors in CBC Waveforms, Tech. Rep. LIGO-T1400682, https://dcc.ligo.org/P1500262/public
Farr, W. M., Sravan, N., Cantrell, A., et al. 2011, ApJ, 741, 103
Farr, W. M., Stevenson, S., Miller, M. C., et al. 2017b, Natur, 548, 426
Hannam, M., Schmidt, P., Bohé, A., et al. 2014, PhRvL, 113, 151101
Healy, J., & Lousto, C. O. 2017, PhRvD, 95, 024037
Hofmann, F., Barausse, E., & Rezzolla, L. 2016, ApJL, 825, L19
Husa, S., Khan, S., Hannam, M., et al. 2016, PhRvD, 93, 044006
Jiménez-Forteza, X., Keitel, D., Husa, S., et al. 2017, PhRvD, 95, 064024
Karki, S., Tuyenbayev, D., Kandhasamy, S., et al. 2016, RScI, 87, 114503
Kasprzack, M., & Yu, H. 2016, Beam Position from Angle to Length minimization, Tech. Rep. LIGO-T1600397, https://dcc.ligo.org/LIGO-T1600397/public
Keitel, D., Jiménez Forteza, X., Husa, S., et al. 2017, PhRvD, 96, 024006
Khan, S., Husa, S., Hannam, M., et al. 2016, PhRvD, 93, 044007
Kidder, L. E. 1995, PhRvD, 52, 821
Klimenko, S., Vedovato, G., Drago, M., et al. 2016, PhRvD, 93, 042004
Krolak, A., & Schutz, B. F. 1987, GReGr, 19, 1163
Lattimer, J. M., & Prakash, M. 2016, PhR, 621, 127
Lipunov, V. M., Kornilov, V., Gorbovskoy, E., et al. 2017, NewA, 51, 122
Littenberg, T. B., & Cornish, N. J. 2015, PhRvD, 91, 084034
Mapelli, M. 2016, MNRAS, 459, 3432
Messick, C., Blackburn, K., Brady, P., et al. 2017, PhRvD, 95, 042001
Mroué, A. H., Scheel, M. A., Szilágyi, B., et al. 2013, PhRvL, 111, 241104
Nitz, A., Harry, I., Brown, D., et al. 2017a, PyCBC software, v1.7.11, Zenodo, doi:10.5281/zenodo.883086, https://ligo-cbc.github.io/
Nitz, A. H., Dent, T., Dal Canton, T., Fairhurst, S., & Brown, D. A. 2017b, ApJ, 849, 118
O'Leary, R. M., Meiron, Y., & Kocsis, B. 2016, ApJL, 824, L12
Özel, F., Psaltis, D., Narayan, R., & McClintock, J. E. 2010, ApJ, 725, 1918
Pretorius, F. 2005, PhRvL, 95, 121101
Pürrer, M. 2016, PhRvD, 93, 064041

Racine, É. 2008, PhRvD, 78, 044021
Rodriguez, C. L., Haster, C.-J., Chatterjee, S., Kalogera, V., & Rasio, F. A. 2016, ApJL, 824, L8
Schmidt, P., Ohme, F., & Hannam, M. 2015, PhRvD, 91, 024043
Schutz, B. F. 2011, CQGra, 28, 125023
Singer, L. P., & Price, L. R. 2016, PhRvD, 93, 024013
Spera, M., Mapelli, M., & Bressan, A. 2015, MNRAS, 451, 4086
Stevenson, S., Berry, C. P. L., & Mandel, I. 2017a, MNRAS, 471, 2801
Stevenson, S., Vigna-Gómez, A., Mandel, I., et al. 2017b, NatCo, 8, 14906
Talbot, C., & Thrane, E. 2017, PhRvD, 96, 023012
Usman, S. A., Nitz, A. H., Harry, I. W., et al. 2016, CQGra, 33, 215004
Veitch, J., Raymond, V., Farr, B., et al. 2015, PhRvD, 91, 042003
Vitale, S., Gerosa, D., Haster, C.-J., Chatziioannou, K., & Zimmerman, A. 2017a, arXiv:1707.04637
Vitale, S., Lynch, R., Sturani, R., & Graff, P. 2017b, CQGra, 34, 03LT01
Was, M., Bizouard, M.-A., Brisson, V., et al. 2010, CQGra, 27, 015005
Zevin, M., Coughlin, S., Bahaadini, S., et al. 2017b, CQGra, 34, 064003
Zevin, M., Pankow, C., Rodriguez, C. L., et al. 2017a, ApJL, 846, 82

B. P. Abbott[1], R. Abbott[1], T. D. Abbott[2], F. Acernese[3,4], K. Ackley[5,6], C. Adams[7], T. Adams[8], P. Addesso[9,10], R. X. Adhikari[1], V. B. Adya[11], C. Affeldt[11], M. Afrough[12], B. Agarwal[13], M. Agathos[14], K. Agatsuma[15], N. Aggarwal[16], O. D. Aguiar[17], L. Aiello[18,19], A. Ain[20], P. Ajith[21], B. Allen[11,22,23], G. Allen[13], A. Allocca[24,25], P. A. Altin[26], A. Amato[27], A. Ananyeva[1], S. B. Anderson[1], W. G. Anderson[22], S. V. Angelova[28], S. Antier[29], S. Appert[1], K. Arai[1], M. C. Araya[1], J. S. Areeda[30], N. Arnaud[29,31], K. G. Arun[32], S. Ascenzi[33,34], G. Ashton[11], M. Ast[35], S. M. Aston[7], P. Astone[36], D. V. Atallah[37], P. Aufmuth[23], C. Aulbert[11], K. AultONeal[38], C. Austin[2], A. Avila-Alvarez[30], S. Babak[39], P. Bacon[40], M. K. M. Bader[15], S. Bae[41], P. T. Baker[42], F. Baldaccini[43,44], G. Ballardin[31], S. W. Ballmer[45], S. Banagiri[46], J. C. Barayoga[1], S. E. Barclay[47], B. C. Barish[1], D. Barker[48], K. Barkett[49], F. Barone[3,4], B. Barr[47], L. Barsotti[16], M. Barsuglia[40], D. Barta[50], J. Bartlett[48], I. Bartos[5,51], R. Bassiri[52], A. Basti[24,25], J. C. Batch[48], M. Bawaj[44,53], J. C. Bayley[47], M. Bazzan[54,55], B. Bécsy[56], C. Beer[11], M. Bejger[57], I. Belahcene[29], A. S. Bell[47], B. K. Berger[1], G. Bergmann[11], J. J. Bero[58], C. P. L. Berry[59], D. Bersanetti[60], A. Bertolini[15], J. Betzwieser[7], S. Bhagwat[45], R. Bhandare[61], I. A. Bilenko[62], G. Billingsley[1], C. R. Billman[5], J. Birch[7], R. Birney[63], O. Birnholtz[11], S. Biscans[1,16], S. Biscoveanu[6,64], A. Bisht[23], M. Bitossi[25,31], C. Biwer[45], M. A. Bizouard[29], J. K. Blackburn[1], J. Blackman[49], C. D. Blair[1,65], D. G. Blair[65], R. M. Blair[48], S. Bloemen[66], O. Bock[11], N. Bode[11], M. Boer[67], G. Bogaert[67], A. Bohe[39], F. Bondu[68], E. Bonilla[52], R. Bonnand[8], B. A. Boom[15], R. Bork[1], V. Boschi[25,31], S. Bose[20,69], K. Bossie[7], Y. Bouffanais[40], A. Bozzi[31], C. Bradaschia[25], P. R. Brady[22], M. Branchesi[18,19], J. E. Brau[70], T. Briant[71], A. Brillet[67], M. Brinkmann[11], V. Brisson[29], P. Brockill[22], J. E. Broida[72], A. F. Brooks[1], D. A. Brown[45], D. D. Brown[73], S. Brunett[1], C. C. Buchanan[2], A. Buikema[16], T. Bulik[74], H. J. Bulten[15,75], A. Buonanno[39,76], D. Buskulic[8], C. Buy[40], R. L. Byer[52], M. Cabero[11], L. Cadonati[77], G. Cagnoli[27,78], C. Cahillane[1], J. Calderón Bustillo[77], T. A. Callister[1], E. Calloni[4,79], J. B. Camp[80], M. Canepa[60,81], P. Canizares[66], K. C. Cannon[82], H. Cao[73], J. Cao[83], C. D. Capano[11], E. Capocasa[40], F. Carbognani[31], S. Caride[84], M. F. Carney[85], J. Casanueva Diaz[29], C. Casentini[33,34], S. Caudill[15,22], M. Cavaglià[12], F. Cavalier[29], R. Cavalieri[31], G. Cella[25], C. B. Cepeda[1], P. Cerdá-Durán[86], G. Cerretani[24,25], E. Cesarini[34,87], S. J. Chamberlin[64], M. Chan[47], S. Chao[88], P. Charlton[89], E. Chase[90], E. Chassande-Mottin[40], D. Chatterjee[22], K. Chatziioannou[91], B. D. Cheeseboro[42], H. Y. Chen[92], X. Chen[65], Y. Chen[49], H.-P. Cheng[5], H. Chia[5], A. Chincarini[60], A. Chiummo[31], T. Chmiel[85], H. S. Cho[93], M. Cho[76], J. H. Chow[26], N. Christensen[67,72], Q. Chu[65], A. J. K. Chua[14], S. Chua[71], A. K. W. Chung[94], S. Chung[65], G. Ciani[5,54,55], R. Ciolfi[95,96], C. E. Cirelli[52], A. Cirone[60,81], F. Clara[48], J. A. Clark[77], P. Clearwater[97], F. Cleva[67], C. Cocchieri[12], E. Coccia[18,19], P.-F. Cohadon[71], D. Cohen[29], A. Colla[36,98], C. G. Collette[99], L. R. Cominsky[100], M. Constancio, Jr.[17], L. Conti[55], S. J. Cooper[59], P. Corban[7], T. R. Corbitt[2], I. Cordero-Carrión[101], K. R. Corley[51], N. Cornish[102], A. Corsi[84], S. Cortese[31], C. A. Costa[17], M. W. Coughlin[1,72], S. B. Coughlin[90], J.-P. Coulon[67], S. T. Countryman[51], P. Couvares[1], P. B. Covas[103], E. E. Cowan[77], D. M. Coward[65], M. J. Cowart[7], D. C. Coyne[1], R. Coyne[84], J. D. E. Creighton[22], T. D. Creighton[104], J. Cripe[2], S. G. Crowder[105], T. J. Cullen[2,30], A. Cumming[47], L. Cunningham[47], E. Cuoco[31], T. Dal Canton[80], G. Dálya[56], S. L. Danilishin[11,23], S. D'Antonio[34], K. Danzmann[11,23], A. Dasgupta[106], C. F. Da Silva Costa[5], V. Dattilo[31], I. Dave[61], M. Davier[29], D. Davis[45], E. J. Daw[107], B. Day[77], S. De[45], D. DeBra[52], J. Degallaix[27], M. De Laurentis[4,18], S. Deléglise[71], W. Del Pozzo[24,25,59], N. Demos[16], T. Denker[11], T. Dent[11], R. De Pietri[108,109], V. Dergachev[39], R. De Rosa[4,79], R. T. DeRosa[7], C. De Rossi[27,31], R. DeSalvo[110], O. de Varona[11], J. Devenson[28], S. Dhurandhar[20], M. C. Díaz[104], L. Di Fiore[4], M. Di Giovanni[96,111], T. Di Girolamo[4,51,79], A. Di Lieto[24,25], S. Di Pace[36,98], I. Di Palma[36,98], F. Di Renzo[24,25], Z. Doctor[92], V. Dolique[27], F. Donovan[16], K. L. Dooley[12], S. Doravari[11], I. Dorrington[37], R. Douglas[47], M. Dovale Álvarez[59], T. P. Downes[22], M. Drago[11], C. Dreissigacker[11], J. C. Driggers[48], Z. Du[83], M. Ducrot[8], P. Dupej[47], S. E. Dwyer[48], T. B. Edo[107], M. C. Edwards[72], A. Effler[7], H.-B. Eggenstein[11,39], P. Ehrens[1], J. Eichholz[1], S. S. Eikenberry[5], R. A. Eisenstein[16], R. C. Essick[16], D. Estevez[8], Z. B. Etienne[42], T. Etzel[1], M. Evans[16], T. M. Evans[7], M. Factourovich[51], V. Fafone[18,33,34], H. Fair[45], S. Fairhurst[37], X. Fan[83], S. Farinon[60], B. Farr[92], W. M. Farr[59], E. J. Fauchon-Jones[37], M. Favata[112], M. Fays[37], C. Fee[85], H. Fehrmann[11], J. Feicht[1], M. M. Fejer[52], A. Fernandez-Galiana[16], I. Ferrante[24,25], E. C. Ferreira[17], F. Ferrini[31], F. Fidecaro[24,25], D. Finstad[45], I. Fiori[31], D. Fiorucci[40], M. Fishbach[92], R. P. Fisher[45], M. Fitz-Axen[46], R. Flaminio[27,113], M. Fletcher[47], H. Fong[91], J. A. Font[86,114], P. W. F. Forsyth[26], S. S. Forsyth[77], J.-D. Fournier[67], S. Frasca[36,98], F. Frasconi[25], Z. Frei[56], A. Freise[59], R. Frey[70], V. Frey[29], E. M. Fries[1], P. Fritschel[16], V. V. Frolov[7], P. Fulda[5], M. Fyffe[7], H. Gabbard[47], B. U. Gadre[20], S. M. Gaebel[59], J. R. Gair[115], L. Gammaitoni[43], M. R. Ganija[73], S. G. Gaonkar[20], C. Garcia-Quiros[103], F. Garufi[4,79], B. Gateley[48], S. Gaudio[38], G. Gaur[116], V. Gayathri[117], N. Gehrels[80,163], G. Gemme[60], E. Genin[31], A. Gennai[25], D. George[13], J. George[61], L. Gergely[118],

V. Germain[8], S. Ghonge[77], Abhirup Ghosh[21], Archisman Ghosh[15,21], S. Ghosh[15,22,66], J. A. Giaime[2,7], K. D. Giardina[7], A. Giazotto[25], K. Gill[38], L. Glover[110], E. Goetz[119], R. Goetz[5], S. Gomes[37], B. Goncharov[6], G. González[2], J. M. Gonzalez Castro[24,25], A. Gopakumar[120], M. L. Gorodetsky[62], S. E. Gossan[1], M. Gosselin[31], R. Gouaty[8], A. Grado[4,121], C. Graef[47], M. Granata[27], A. Grant[47], S. Gras[16], C. Gray[48], G. Greco[122,123], A. C. Green[59], E. M. Gretarsson[38], P. Groot[66], H. Grote[11], S. Grunewald[39], P. Gruning[29], G. M. Guidi[122,123], X. Guo[83], A. Gupta[64], M. K. Gupta[106], K. E. Gushwa[1], E. K. Gustafson[1], R. Gustafson[119], O. Halim[18,19], B. R. Hall[69], E. D. Hall[16], E. Z. Hamilton[37], G. Hammond[47], M. Haney[124], M. M. Hanke[11], J. Hanks[48], C. Hanna[64], M. D. Hannam[37], O. A. Hannuksela[94], J. Hanson[7], T. Hardwick[2], J. Harms[18,19], G. M. Harry[125], I. W. Harry[39], M. J. Hart[47], C.-J. Haster[91], K. Haughian[47], J. Healy[58], A. Heidmann[71], M. C. Heintze[7], H. Heitmann[67], P. Hello[29], G. Hemming[31], M. Hendry[47], I. S. Heng[47], J. Hennig[47], A. W. Heptonstall[1], M. Heurs[11,23], S. Hild[47], T. Hinderer[66], D. Hoak[31], D. Hofman[27], K. Holt[7], D. E. Holz[92], P. Hopkins[37], C. Horst[22], J. Hough[47], E. A. Houston[47], E. J. Howell[65], A. Hreibi[67], Y. M. Hu[11], E. A. Huerta[13], D. Huet[29], B. Hughey[38], S. Husa[103], S. H. Huttner[47], T. Huynh-Dinh[7], N. Indik[11], R. Inta[84], G. Intini[36,98], H. N. Isa[47], J.-M. Isac[71], M. Isi[1], B. R. Iyer[21], K. Izumi[48], T. Jacqmin[71], K. Jani[77], P. Jaranowski[126], S. Jawahar[63], F. Jiménez-Forteza[103], W. W. Johnson[2], N. K. Johnson-McDaniel[14], D. I. Jones[127], R. Jones[47], R. J. G. Jonker[15], L. Ju[65], J. Junker[11], C. V. Kalaghatgi[37], V. Kalogera[90], B. Kamai[1], S. Kandhasamy[7], G. Kang[41], J. B. Kanner[1], S. J. Kapadia[22], S. Karki[70], K. S. Karvinen[11], M. Kasprzack[2], M. Katolik[13], E. Katsavounidis[16], W. Katzman[7], S. Kaufer[23], K. Kawabe[48], F. Kéfélian[67], D. Keitel[47], A. J. Kemball[13], R. Kennedy[107], C. Kent[37], J. S. Key[128], F. Y. Khalili[62], I. Khan[18,34], S. Khan[11], Z. Khan[106], E. A. Khazanov[129], N. Kijbunchoo[26], Chunglee Kim[130], J. C. Kim[131], K. Kim[94], W. Kim[73], W. S. Kim[132], Y.-M. Kim[93], S. J. Kimbrell[77], E. J. King[73], P. J. King[48], M. Kinley-Hanlon[125], R. Kirchhoff[11], J. S. Kissel[48], L. Kleybolte[35], S. Klimenko[5], T. D. Knowles[42], P. Koch[11], S. M. Koehlenbeck[11], S. Koley[15], V. Kondrashov[1], A. Kontos[16], M. Korobko[35], W. Z. Korth[1], I. Kowalska[74], D. B. Kozak[1], C. Krämer[11], V. Kringel[11], B. Krishnan[11], A. Królak[133,134], G. Kuehn[11], P. Kumar[91], R. Kumar[106], S. Kumar[21], L. Kuo[88], A. Kutynia[133], S. Kwang[22], B. D. Lackey[39], K. H. Lai[94], M. Landry[48], R. N. Lang[135], J. Lange[58], B. Lantz[52], R. K. Lanza[16], A. Lartaux-Vollard[29], P. D. Lasky[6], M. Laxen[7], A. Lazzarini[1], C. Lazzaro[55], P. Leaci[36,98], S. Leavey[47], C. H. Lee[93], H. K. Lee[136], H. M. Lee[137], H. W. Lee[131], K. Lee[47], J. Lehmann[11], A. Lenon[42], M. Leonardi[96,111], N. Leroy[29], N. Letendre[8], Y. Levin[6], T. G. F. Li[94], S. D. Linker[110], T. B. Littenberg[138], J. Liu[65], R. K. L. Lo[94], N. A. Lockerbie[63], L. T. London[37], J. E. Lord[45], M. Lorenzini[18,19], V. Loriette[139], M. Lormand[7], G. Losurdo[25], J. D. Lough[11], C. O. Lousto[58], G. Lovelace[30], H. Lück[11,23], D. Lumaca[33,34], A. P. Lundgren[11], R. Lynch[16], Y. Ma[49], R. Macas[37], S. Macfoy[28], B. Machenschalk[11], M. MacInnis[16], D. M. Macleod[37], I. Magaña Hernandez[22], F. Magaña-Sandoval[45], L. Magaña Zertuche[45], R. M. Magee[64], E. Majorana[36], I. Maksimovic[139], N. Man[67], V. Mandic[46], V. Mangano[47], G. L. Mansell[26], M. Manske[22,26], M. Mantovani[31], F. Marchesoni[44,53], F. Marion[8], S. Márka[51], Z. Márka[51], C. Markakis[13], A. S. Markosyan[52], A. Markowitz[1], E. Maros[1], A. Marquina[101], F. Martelli[122,123], L. Martellini[67], I. W. Martin[47], R. M. Martin[112], D. V. Martynov[16], K. Mason[16], E. Massera[107], A. Masserot[8], T. J. Massinger[1], M. Masso-Reid[47], S. Mastrogiovanni[36,98], A. Matas[46], F. Matichard[1,16], L. Matone[51], N. Mavalvala[16], N. Mazumder[69], R. McCarthy[48], D. E. McClelland[26], S. McCormick[7], L. McCuller[16], S. C. McGuire[140], G. McIntyre[1], J. McIver[1], D. J. McManus[26], L. McNeill[6], T. McRae[26], S. T. McWilliams[42], D. Meacher[64], G. D. Meadors[11,39], M. Mehmet[11], J. Meidam[15], E. Mejuto-Villa[9,10], A. Melatos[97], G. Mendell[48], R. A. Mercer[22], E. L. Merilh[48], M. Merzougui[67], S. Meshkov[1], C. Messenger[47], C. Messick[64], R. Metzdorff[71], P. M. Meyers[46], H. Miao[59], C. Michel[27], H. Middleton[59], E. E. Mikhailov[141], L. Milano[4,79], A. L. Miller[5,36,98], B. B. Miller[90], J. Miller[16], M. Millhouse[102], M. C. Milovich-Goff[110], O. Minazzoli[67,142], Y. Minenkov[34], J. Ming[39], C. Mishra[143], S. Mitra[20], V. P. Mitrofanov[62], G. Mitselmakher[5], R. Mittleman[16], D. Moffa[85], A. Moggi[25], K. Mogushi[12], M. Mohan[31], S. R. P. Mohapatra[16], M. Montani[122,123], C. J. Moore[14], D. Moraru[48], G. Moreno[48], S. R. Morriss[104], B. Mours[8], C. M. Mow-Lowry[59], G. Mueller[5], A. W. Muir[37], Arunava Mukherjee[11], D. Mukherjee[22], S. Mukherjee[104], N. Mukund[20], A. Mullavey[7], J. Munch[73], E. A. Muñiz[45], M. Muratore[38], P. G. Murray[47], K. Napier[77], I. Nardecchia[33,34], L. Naticchioni[36,98], R. K. Nayak[144], J. Neilson[110], G. Nelemans[15,66], T. J. N. Nelson[7], M. Nery[11], A. Neunzert[119], L. Nevin[1], J. M. Newport[125], G. Newton[47,164], K. K. Y. Ng[94], T. T. Nguyen[26], D. Nichols[66], A. B. Nielsen[11], S. Nissanke[15,66], A. Nitz[11], A. Noack[11], F. Nocera[31], D. Nolting[7], C. North[37], L. K. Nuttall[37], J. Oberling[48], G. D. O'Dea[110], G. H. Ogin[145], J. J. Oh[132], S. H. Oh[132], F. Ohme[11], M. A. Okada[17], M. Oliver[103], P. Oppermann[11], Richard J. Oram[7], B. O'Reilly[7], R. Ormiston[46], L. F. Ortega[5], R. O'Shaughnessy[58], S. Ossokine[39], D. J. Ottaway[73], H. Overmier[7], B. J. Owen[84], A. E. Pace[64], J. Page[138], M. A. Page[65], A. Pai[117,146], S. A. Pai[61], J. R. Palamos[70], O. Palashov[129], C. Palomba[36], A. Pal-Singh[35], Howard Pan[88], Huang-Wei Pan[88], B. Pang[49], P. T. H. Pang[94], C. Pankow[90], F. Pannarale[37], B. C. Pant[61], F. Paoletti[25], A. Paoli[31], M. A. Papa[11,22,39], A. Parida[20], W. Parker[7], D. Pascucci[47], A. Pasqualetti[31], R. Passaquieti[24,25], D. Passuello[25], M. Patil[134], B. Patricelli[25,147], B. L. Pearlstone[47], M. Pedraza[1], R. Pedurand[27,148], L. Pekowsky[45], A. Pele[7], S. Penn[149], C. J. Perez[48], A. Perreca[1,96,111], L. M. Perri[90], H. P. Pfeiffer[39,91], M. Phelps[47], O. J. Piccinni[36,98], M. Pichot[67], F. Piergiovanni[122,123], V. Pierro[9,10], G. Pillant[31], L. Pinard[27], I. M. Pinto[9,10], M. Pirello[48], M. Pitkin[47], M. Poe[22], R. Poggiani[24,25], P. Popolizio[31], E. K. Porter[40], A. Post[11], J. Powell[47,150], J. Prasad[20], J. W. W. Pratt[38], G. Pratten[103], V. Predoi[37], T. Prestegard[22], M. Prijatelj[11], M. Principe[9,10], S. Privitera[39], G. A. Prodi[96,111], L. G. Prokhorov[62], O. Puncken[11], M. Punturo[44], P. Puppo[36], M. Pürrer[39], H. Qi[22], V. Quetschke[104], E. A. Quintero[1], R. Quitzow-James[70], F. J. Raab[48], D. S. Rabeling[26], H. Radkins[48], P. Raffai[56], S. Raja[61], C. Rajan[61], B. Rajbhandari[84], M. Rakhmanov[104], K. E. Ramirez[104], A. Ramos-Buades[103], P. Rapagnani[36,98],

V. Raymond[39], M. Razzano[24,25], J. Read[30], T. Regimbau[67], L. Rei[60], S. Reid[63], D. H. Reitze[1,5], W. Ren[13], S. D. Reyes[45], F. Ricci[36,98], P. M. Ricker[13], S. Rieger[11], K. Riles[119], M. Rizzo[58], N. A. Robertson[1,47], R. Robie[47], F. Robinet[29], A. Rocchi[34], L. Rolland[8], J. G. Rollins[1], V. J. Roma[70], R. Romano[3,4], C. L. Romel[48], J. H. Romie[7], D. Rosińska[57,151], M. P. Ross[152], S. Rowan[47], A. Rüdiger[11], P. Ruggi[31], G. Rutins[28], K. Ryan[48], S. Sachdev[1], T. Sadecki[48], L. Sadeghian[22], M. Sakellariadou[153], L. Salconi[31], M. Saleem[117], F. Salemi[11], A. Samajdar[144], L. Sammut[6], L. M. Sampson[90], E. J. Sanchez[1], L. E. Sanchez[1], N. Sanchis-Gual[86], V. Sandberg[48], J. R. Sanders[45], B. Sassolas[27], B. S. Sathyaprakash[37,64], P. R. Saulson[45], O. Sauter[119], R. L. Savage[48], A. Sawadsky[35], P. Schale[70], M. Scheel[49], J. Scheuer[90], J. Schmidt[11], P. Schmidt[1,66], R. Schnabel[35], R. M. S. Schofield[70], A. Schönbeck[35], E. Schreiber[11], D. Schuette[11,23], B. W. Schulte[11], B. F. Schutz[11,37], S. G. Schwalbe[38], J. Scott[47], S. M. Scott[26], E. Seidel[13], D. Sellers[7], A. S. Sengupta[154], D. Sentenac[31], V. Sequino[18,33,34], A. Sergeev[129], D. A. Shaddock[26], T. J. Shaffer[48], A. A. Shah[138], M. S. Shahriar[90], M. B. Shaner[110], L. Shao[39], B. Shapiro[52], P. Shawhan[76], A. Sheperd[22], D. H. Shoemaker[16], D. M. Shoemaker[77], K. Siellez[77], X. Siemens[22], M. Sieniawska[57], D. Sigg[48], A. D. Silva[17], L. P. Singer[80], A. Singh[11,23,39], A. Singhal[18,36], A. M. Sintes[103], B. J. J. Slagmolen[26], B. Smith[7], J. R. Smith[30], R. J. E. Smith[1,6], S. Somala[155], E. J. Son[132], J. A. Sonnenberg[22], B. Sorazu[47], F. Sorrentino[60], T. Souradeep[20], A. P. Spencer[47], A. K. Srivastava[106], K. Staats[38], A. Staley[51], M. Steinke[11], J. Steinlechner[35,47], S. Steinlechner[35], D. Steinmeyer[11], S. P. Stevenson[59,150], R. Stone[104], D. J. Stops[59], K. A. Strain[47], G. Stratta[122,123], S. E. Strigin[62], A. Strunk[48], R. Sturani[156], A. L. Stuver[7], T. Z. Summerscales[157], L. Sun[97], S. Sunil[106], J. Suresh[20], P. J. Sutton[37], B. L. Swinkels[31], M. J. Szczepańczyk[38], M. Tacca[15], S. C. Tait[47], C. Talbot[6], D. Talukder[70], D. B. Tanner[5], M. Tápai[118], A. Taracchini[39], J. D. Tasson[72], J. A. Taylor[138], R. Taylor[1], S. V. Tewari[149], T. Theeg[11], F. Thies[11], E. G. Thomas[59], M. Thomas[7], P. Thomas[48], K. A. Thorne[7], E. Thrane[6], S. Tiwari[18,96], V. Tiwari[37], K. V. Tokmakov[63], K. Toland[47], M. Tonelli[24,25], Z. Tornasi[47], A. Torres-Forné[86], C. I. Torrie[1], D. Töyrä[59], F. Travasso[31,44], G. Traylor[7], J. Trinastic[5], M. C. Tringali[96,111], L. Trozzo[25,158], K. W. Tsang[15], M. Tse[16], R. Tso[1], L. Tsukada[82], D. Tsuna[82], D. Tuyenbayev[104], K. Ueno[22], D. Ugolini[159], C. S. Unnikrishnan[120], A. L. Urban[1], S. A. Usman[37], H. Vahlbruch[23], G. Vajente[1], G. Valdes[2], N. van Bakel[15], M. van Beuzekom[15], J. F. J. van den Brand[15,75], C. Van Den Broeck[15,160], D. C. Vander-Hyde[45], L. van der Schaaf[15], J. V. van Heijningen[15], A. A. van Veggel[47], M. Vardaro[54,55], V. Varma[49], S. Vass[1], M. Vasúth[50], A. Vecchio[59], G. Vedovato[55], J. Veitch[47], P. J. Veitch[73], K. Venkateswara[152], G. Venugopalan[1], D. Verkindt[8], F. Vetrano[122,123], A. Viceré[122,123], A. D. Viets[22], S. Vinciguerra[59], D. J. Vine[28], J.-Y. Vinet[67], S. Vitale[16], T. Vo[45], H. Vocca[43,44], C. Vorvick[48], S. P. Vyatchanin[62], A. R. Wade[1], L. E. Wade[85], M. Wade[85], R. Walet[15], M. Walker[30], L. Wallace[1], S. Walsh[11,22,39], G. Wang[18,123], H. Wang[59], J. Z. Wang[64], W. H. Wang[104], Y. F. Wang[94], R. L. Ward[26], J. Warner[48], M. Was[8], J. Watchi[99], B. Weaver[48], L.-W. Wei[11,23], M. Weinert[11], A. J. Weinstein[1], R. Weiss[16], L. Wen[65], E. K. Wessel[13], P. Weßels[11], J. Westerweck[11], T. Westphal[11], K. Wette[26], J. T. Whelan[58], B. F. Whiting[5], C. Whittle[6], D. Wilken[11], D. Williams[47], R. D. Williams[1], A. R. Williamson[66], J. L. Willis[1,161], B. Willke[11,23], M. H. Wimmer[11], W. Winkler[11], C. C. Wipf[1], H. Wittel[11,23], G. Woan[47], J. Woehler[11], J. Wofford[58], K. W. K. Wong[94], J. Worden[48], J. L. Wright[47], D. S. Wu[11], D. M. Wysocki[58], S. Xiao[1], H. Yamamoto[1], C. C. Yancey[76], L. Yang[162], M. J. Yap[26], M. Yazback[5], Hang Yu[16], Haocun Yu[16], M. Yvert[8], A. Zadrożny[133], M. Zanolin[38], T. Zelenova[31], J.-P. Zendri[55], M. Zevin[90], L. Zhang[1], M. Zhang[141], T. Zhang[47], Y.-H. Zhang[58], C. Zhao[65], M. Zhou[90], Z. Zhou[90], S. J. Zhu[11,39], X. J. Zhu[6], A. B. Zimmerman[91], M. E. Zucker[1,16], and J. Zweizig[1]

(LIGO Scientific Collaboration and Virgo Collaboration)

[1] LIGO, California Institute of Technology, Pasadena, CA 91125, USA
[2] Louisiana State University, Baton Rouge, LA 70803, USA
[3] Università di Salerno, Fisciano, I-84084 Salerno, Italy
[4] INFN, Sezione di Napoli, Complesso Universitario di Monte S.Angelo, I-80126 Napoli, Italy
[5] University of Florida, Gainesville, FL 32611, USA
[6] OzGrav, School of Physics & Astronomy, Monash University, Clayton, Victoria, 3800, Australia
[7] LIGO Livingston Observatory, Livingston, LA 70754, USA
[8] Laboratoire d'Annecy-le-Vieux de Physique des Particules (LAPP), Université Savoie Mont Blanc, CNRS/IN2P3, F-74941 Annecy, France
[9] University of Sannio at Benevento, I-82100 Benevento, Italy
[10] INFN, Sezione di Napoli, I-80100 Napoli, Italy
[11] Max Planck Institute for Gravitational Physics (Albert Einstein Institute), D-30167 Hannover, Germany
[12] The University of Mississippi, University, MS 38677, USA
[13] NCSA, University of Illinois at Urbana-Champaign, Urbana, IL 61801, USA
[14] University of Cambridge, Cambridge CB2 1TN, UK
[15] Nikhef, Science Park, 1098 XG Amsterdam, The Netherlands
[16] LIGO, Massachusetts Institute of Technology, Cambridge, MA 02139, USA
[17] Instituto Nacional de Pesquisas Espaciais, José dos Campos, São Paulo 12227-010 São, Brazil
[18] Gran Sasso Science Institute (GSSI), I-67100 L'Aquila, Italy
[19] INFN, Laboratori Nazionali del Gran Sasso, I-67100 Assergi, Italy
[20] Inter-University Centre for Astronomy and Astrophysics, Pune 411007, India
[21] International Centre for Theoretical Sciences, Tata Institute of Fundamental Research, Bengaluru 560089, India
[22] University of Wisconsin-Milwaukee, Milwaukee, WI 53201, USA
[23] Leibniz Universität Hannover, D-30167 Hannover, Germany
[24] Università di Pisa, I-56127 Pisa, Italy
[25] INFN, Sezione di Pisa, I-56127 Pisa, Italy
[26] OzGrav, Australian National University, Canberra, ACT 0200, Australia
[27] Laboratoire des Matériaux Avancés (LMA), CNRS/IN2P3, F-69622 Villeurbanne, France

[28] SUPA, University of the West of Scotland, Paisley PA1 2BE, UK
[29] LAL, Univ. Paris-Sud, CNRS/IN2P3, Université Paris-Saclay, F-91898 Orsay, France
[30] California State University Fullerton, Fullerton, CA 92831, USA
[31] European Gravitational Observatory (EGO), I-56021 Cascina, Pisa, Italy
[32] Chennai Mathematical Institute, Chennai 603103, India
[33] Università di Roma Tor Vergata, I-00133 Roma, Italy
[34] INFN, Sezione di Roma Tor Vergata, I-00133 Roma, Italy
[35] Universität Hamburg, D-22761 Hamburg, Germany
[36] INFN, Sezione di Roma, I-00185 Roma, Italy
[37] Cardiff University, Cardiff CF24 3AA, UK
[38] Embry-Riddle Aeronautical University, Prescott, AZ 86301, USA
[39] Max Planck Institute for Gravitational Physics (Albert Einstein Institute), D-14476 Potsdam-Golm, Germany
[40] APC, AstroParticule et Cosmologie, Université Paris Diderot, CNRS/IN2P3, CEA/Irfu, Observatoire de Paris, Sorbonne Paris Cité, F-75205 Paris Cedex 13, France
[41] Korea Institute of Science and Technology Information, Daejeon 34141, Korea
[42] West Virginia University, Morgantown, WV 26506, USA
[43] Università di Perugia, I-06123 Perugia, Italy
[44] INFN, Sezione di Perugia, I-06123 Perugia, Italy
[45] Syracuse University, Syracuse, NY 13244, USA
[46] University of Minnesota, Minneapolis, MN 55455, USA
[47] SUPA, University of Glasgow, Glasgow G12 8QQ, UK
[48] LIGO Hanford Observatory, Richland, WA 99352, USA
[49] Caltech CaRT, Pasadena, CA 91125, USA
[50] Wigner RCP, RMKI, H-1121 Budapest, Konkoly Thege Miklós út 29-33, Hungary
[51] Columbia University, New York, NY 10027, USA
[52] Stanford University, Stanford, CA 94305, USA
[53] Università di Camerino, Dipartimento di Fisica, I-62032 Camerino, Italy
[54] Università di Padova, Dipartimento di Fisica e Astronomia, I-35131 Padova, Italy
[55] INFN, Sezione di Padova, I-35131 Padova, Italy
[56] Institute of Physics, Eötvös University, Pázmány P.s. 1/A, Budapest 1117, Hungary
[57] Nicolaus Copernicus Astronomical Center, Polish Academy of Sciences, 00-716, Warsaw, Poland
[58] Rochester Institute of Technology, Rochester, NY 14623, USA
[59] University of Birmingham, Birmingham B15 2TT, UK
[60] INFN, Sezione di Genova, I-16146 Genova, Italy
[61] RRCAT, Indore MP 452013, India
[62] Faculty of Physics, Lomonosov Moscow State University, Moscow 119991, Russia
[63] SUPA, University of Strathclyde, Glasgow G1 1XQ, UK
[64] The Pennsylvania State University, University Park, PA 16802, USA
[65] OzGrav, University of Western Australia, Crawley, Western Australia 6009, Australia
[66] Department of Astrophysics/IMAPP, Radboud University Nijmegen, P.O. Box 9010, 6500 GL Nijmegen, The Netherlands
[67] Artemis, Université Côte d'Azur, Observatoire Côte d'Azur, CNRS, CS 34229, F-06304 Nice Cedex 4, France
[68] Institut FOTON, CNRS, Université de Rennes 1, F-35042 Rennes, France
[69] Washington State University, Pullman, WA 99164, USA
[70] University of Oregon, Eugene, OR 97403, USA
[71] Laboratoire Kastler Brossel, UPMC-Sorbonne Universités, CNRS, ENS-PSL Research University, Collège de France, F-75005 Paris, France
[72] Carleton College, Northfield, MN 55057, USA
[73] OzGrav, University of Adelaide, Adelaide, South Australia 5005, Australia
[74] Astronomical Observatory Warsaw University, 00-478 Warsaw, Poland
[75] VU University Amsterdam, 1081 HV Amsterdam, The Netherlands
[76] University of Maryland, College Park, MD 20742, USA
[77] School of Physics, Georgia Institute of Technology, Atlanta, GA 30332, USA
[78] Université Claude Bernard Lyon 1, F-69622 Villeurbanne, France
[79] Università di Napoli "Federico II," Complesso Universitario di Monte S.Angelo, I-80126 Napoli, Italy
[80] NASA Goddard Space Flight Center, Greenbelt, MD 20771, USA
[81] Dipartimento di Fisica, Università degli Studi di Genova, I-16146 Genova, Italy
[82] RESCEU, University of Tokyo, Tokyo 113-0033, Japan
[83] Tsinghua University, Beijing 100084, People's Republic of China
[84] Texas Tech University, Lubbock, TX 79409, USA
[85] Kenyon College, Gambier, OH 43022, USA
[86] Departamento de Astronomía y Astrofísica, Universitat de València, E-46100 Burjassot, València, Spain
[87] Museo Storico della Fisica e Centro Studi e Ricerche Enrico Fermi, I-00184 Roma, Italy
[88] National Tsing Hua University, Hsinchu City, 30013 Taiwan, People's Republic of China
[89] Charles Sturt University, Wagga Wagga, NSW 2678, Australia
[90] Center for Interdisciplinary Exploration & Research in Astrophysics (CIERA), Northwestern University, Evanston, IL 60208, USA
[91] Canadian Institute for Theoretical Astrophysics, University of Toronto, Toronto, Ontario M5S 3H8, Canada
[92] University of Chicago, Chicago, IL 60637, USA
[93] Pusan National University, Busan 46241, Korea
[94] The Chinese University of Hong Kong, Shatin, NT, Hong Kong
[95] INAF, Osservatorio Astronomico di Padova, I-35122 Padova, Italy
[96] INFN, Trento Institute for Fundamental Physics and Applications, I-38123 Povo, Trento, Italy
[97] OzGrav, University of Melbourne, Parkville, Victoria 3010, Australia
[98] Università di Roma "La Sapienza," I-00185 Roma, Italy
[99] Université Libre de Bruxelles, Brussels B-1050, Belgium
[100] Sonoma State University, Rohnert Park, CA 94928, USA
[101] Departamento de Matemáticas, Universitat de València, E-46100 Burjassot, València, Spain

[102] Montana State University, Bozeman, MT 59717, USA
[103] Universitat de les Illes Balears, IAC3—IEEC, E-07122 Palma de Mallorca, Spain
[104] The University of Texas Rio Grande Valley, Brownsville, TX 78520, USA
[105] Bellevue College, Bellevue, WA 98007, USA
[106] Institute for Plasma Research, Bhat, Gandhinagar 382428, India
[107] The University of Sheffield, Sheffield S10 2TN, UK
[108] Dipartimento di Scienze Matematiche, Fisiche e Informatiche, Università di Parma, I-43124 Parma, Italy
[109] INFN, Sezione di Milano Bicocca, Gruppo Collegato di Parma, I-43124 Parma, Italy
[110] California State University, Los Angeles, 5151 State University Dr, Los Angeles, CA 90032, USA
[111] Università di Trento, Dipartimento di Fisica, I-38123 Povo, Trento, Italy
[112] Montclair State University, Montclair, NJ 07043, USA
[113] National Astronomical Observatory of Japan, 2-21-1 Osawa, Mitaka, Tokyo 181-8588, Japan
[114] Observatori Astronòmic, Universitat de València, E-46980 Paterna, València, Spain
[115] School of Mathematics, University of Edinburgh, Edinburgh EH9 3FD, UK
[116] University and Institute of Advanced Research, Koba Institutional Area, Gandhinagar Gujarat 382007, India
[117] IISER-TVM, CET Campus, Trivandrum Kerala 695016, India
[118] University of Szeged, Dóm tér 9, Szeged 6720, Hungary
[119] University of Michigan, Ann Arbor, MI 48109, USA
[120] Tata Institute of Fundamental Research, Mumbai 400005, India
[121] INAF, Osservatorio Astronomico di Capodimonte, I-80131, Napoli, Italy
[122] Università degli Studi di Urbino "Carlo Bo," I-61029 Urbino, Italy
[123] INFN, Sezione di Firenze, I-50019 Sesto Fiorentino, Firenze, Italy
[124] Physik-Institut, University of Zurich, Winterthurerstrasse 190, 8057 Zurich, Switzerland
[125] American University, Washington, DC 20016, USA
[126] University of Białystok, 15-424 Białystok, Poland
[127] University of Southampton, Southampton SO17 1BJ, UK
[128] University of Washington Bothell, 18115 Campus Way NE, Bothell, WA 98011, USA
[129] Institute of Applied Physics, Nizhny Novgorod, 603950, Russia
[130] Korea Astronomy and Space Science Institute, Daejeon 34055, Korea
[131] Inje University Gimhae, South Gyeongsang 50834, Korea
[132] National Institute for Mathematical Sciences, Daejeon 34047, Korea
[133] NCBJ, 05-400 Świerk-Otwock, Poland
[134] Institute of Mathematics, Polish Academy of Sciences, 00656 Warsaw, Poland
[135] Hillsdale College, Hillsdale, MI 49242, USA
[136] Hanyang University, Seoul 04763, Korea
[137] Seoul National University, Seoul 08826, Korea
[138] NASA Marshall Space Flight Center, Huntsville, AL 35811, USA
[139] ESPCI, CNRS, F-75005 Paris, France
[140] Southern University and A&M College, Baton Rouge, LA 70813, USA
[141] College of William and Mary, Williamsburg, VA 23187, USA
[142] Centre Scientifique de Monaco, 8 quai Antoine Ier, MC-98000, Monaco
[143] Indian Institute of Technology Madras, Chennai 600036, India
[144] IISER-Kolkata, Mohanpur, West Bengal 741252, India
[145] Whitman College, 345 Boyer Avenue, Walla Walla, WA 99362, USA
[146] Indian Institute of Technology Bombay, Powai, Mumbai, Maharashtra 400076, India
[147] Scuola Normale Superiore, Piazza dei Cavalieri 7, I-56126 Pisa, Italy
[148] Université de Lyon, F-69361 Lyon, France
[149] Hobart and William Smith Colleges, Geneva, NY 14456, USA
[150] OzGrav, Swinburne University of Technology, Hawthorn, VIC 3122, Australia
[151] Janusz Gil Institute of Astronomy, University of Zielona Góra, 65-265 Zielona Góra, Poland
[152] University of Washington, Seattle, WA 98195, USA
[153] King's College London, University of London, London WC2R 2LS, UK
[154] Indian Institute of Technology, Gandhinagar Ahmedabad Gujarat 382424, India
[155] Indian Institute of Technology Hyderabad, Sangareddy, Khandi, Telangana 502285, India
[156] International Institute of Physics, Universidade Federal do Rio Grande do Norte, Natal RN 59078-970, Brazil
[157] Andrews University, Berrien Springs, MI 49104, USA
[158] Università di Siena, I-53100 Siena, Italy
[159] Trinity University, San Antonio, TX 78212, USA
[160] Van Swinderen Institute for Particle Physics and Gravity, University of Groningen, Nijenborgh 4, 9747 AG Groningen, The Netherlands
[161] Abilene Christian University, Abilene, TX 79699, USA
[162] Colorado State University, Fort Collins, CO 80523, USA
[163] Deceased, 2017 February.
[164] Deceased, 2016 December.